Group B Streptococcus Adaptation Promotes Survival in a Hyper-inflammatory Diabetic Wound Environment

Rebecca A. Keogh[1], Amanda L. Haeberle[1], Christophe J. Langouët-Astrié[2], Jeffrey S. Kavanaugh[1], Eric P. Schmidt[2], Garrett D. Moore[4], Alexander R. Horswill[1,3]* and Kelly S. Doran[1]*.

[1]Department of Immunology and Microbiology, University of Colorado Anschutz, Aurora, CO, USA

[2]Department of Medicine- Pulmonary Sciences and Critical Care, University of Colorado Anschutz, Aurora, CO, USA

[3]Department of Veterans Affairs Eastern Colorado Healthcare System, Aurora, Colorado, USA.

[4]Department of Orthopedics, University of Colorado, Anschutz Medical Campus, Aurora, CO, USA

*Corresponding authors: Alexander R. Horswill and Kelly S. Doran, Department of Immunology and Microbiology, University of Colorado School of Medicine, Anschutz Medical Campus 12800 East 19th Avenue Aurora, CO, USA. Phone: (303) 724-3539, Fax: (303) 724-4226, E-mail: kelly.doran@cuanschutz.edu

Running title: GBS Adaptation in the Diabetic Wound

Abstract

Diabetic wounds have poor healing outcomes due to the presence of numerous pathogens and a dysregulated immune response. Group B *Streptococcus* (GBS) is commonly isolated from diabetic wound infections, but the mechanisms of GBS virulence during these infections have not been investigated. Here, we develop a murine model of GBS diabetic wound infection, and using dual RNA-sequencing, demonstrate that GBS infection triggers an inflammatory response. GBS adapts to this hyperinflammatory environment by upregulating virulence factors including those known to be regulated by the the two-component system *covRS*, such as the surface protein *pbsP*, and the *cyl* operon which is responsible for hemolysin/pigmentation production. We recover hyper-pigmented/hemolytic GBS colonies from the murine diabetic wound which we determined encode mutations in *covR*. We further demonstrate that GBS mutants in *cylE* and *pbsP* are attenuated in the diabetic wound. This foundational study provides insight into the pathogenesis of GBS diabetic wound infections.

Introduction

Diabetes is a multifaceted metabolic disease that is estimated to affect more than 500 million individuals worldwide by 2035 (1). One of the most common complications in diabetic individuals is the development of wounds such as foot ulcers, which an estimated 19-34% of all patients will develop in their lifetime (2). Normal wound healing progresses in four overlapping stages; (i) hemostasis, (ii) inflammation, (iii) proliferation and (iv) remodeling (3). However, diabetic wounds are often stalled in a state of chronic inflammation, and cannot progress through the later stages of healing (4–6). A hallmark characteristic of chronic inflammation is excess infiltration of neutrophils and macrophages. Leukocyte abundance can be harmful to wound healing due to high production of reactive oxygen species and serine proteases, which degrade structural proteins of the extracellular matrix therefore limiting proliferation and remodeling (7). In addition, diabetic wounds are colonized with numerous bacterial pathogens that trigger leukocyte influx and exacerbate poor healing outcomes (8).

Some of the most common species isolated from chronic wounds are *Staphylococcus aureus*, *Pseudomonas aeruginosa* and *Streptococcus agalactiae*, also known as Group B *Streptococcus* (GBS) (9–12). *S. aureus* is responsible for 76% of all skin and soft tissue infections and is found in wounds of both non-diabetic and diabetic individuals (11, 13). Thurlow et al. has shown that elevated glucose in hyperglycemic abscesses leads to increased virulence potential of *S. aureus*, and is dependent on two glucose transporters (14). In addition, specific *S. aureus* factors such as the proteases ClpX, ClpP and ClpC were shown to contribute to *S. aureus* skin infection in diabetic mice (15). *P. aeruginosa* is also a commonly isolated bacterium from wounds of both non-diabetic and diabetic individuals (11, 16). *P. aeruginosa* infection of chronic wounds has been linked to enhanced biofilm formation and activation of

matrix metalloproteases that degrade extracellular matrix molecules (17, 18). Conversely, GBS is rarely identified from non-diabetic wounds, but is being increasingly identified in diabetic individuals (19, 20). While some work has characterized *S. aureus* and *P. aeruginosa* in diabetic wound infections, no previous studies have investigated GBS pathogenesis in the diabetic wound or on the skin in general. In addition, little is known about the mechanisms by which bacteria survive inflammation in the diabetic wound environment.

GBS is an opportunistic pathogen that is a leading cause of neonatal invasive infections. Approximately 20-30% of pregnant women are colonized with GBS in the vaginal tract, and can transmit this bacterium to the neonate *in utero* or during birth (21, 22). Neonatal infections can lead to the development of invasive diseases like sepsis, pneumonia and meningitis, with a mortality rate of 10-15% (23). In addition to neonatal infections, GBS infection of non-pregnant adults, including the immunocompromised is on the rise, with over two-thirds of invasive GBS disease occurring in adults (24). Of these individuals, the most common comorbidity is diabetes, which is present in 20-25% of nonpregnant adults with GBS (24). Despite this, the majority of GBS studies have focused on vaginal colonization and neonatal disease; and the mechanisms of GBS pathogenesis in diabetic infection have not been examined.

Numerous reports have identified mechanisms of GBS colonization that contribute to vaginal persistence, as well as mechanisms of invasive infection such as systemic disease and meningitis. GBS produces multiple virulence factors, including the β-hemolysin/carotenoid pigment (encoded by *cylE*), various surface adhesins such as pili, serine-rich repeat (Srr) proteins and BspC that bind host extracellular matrix proteins (ECMs) and receptors to promote adherence and invasion, as well as immune evasion factors such as the polysaccharide capsule, that allows the bacterium to resist phagocytic killing and persist in the human host (25–29). Ten

capsular serotypes have been identified, with serotypes Ia, Ib, II, III and V being the most common serotypes associated with disease (30). The transition from a commensal lifestyle to infection is controlled by multiple regulators such as transcription factors and two-component systems (TCS) that coordinate the expression of these virulence factors in the host. TCS typically encode a sensor histidine kinase which recognizes a stimulus and a cognate response regulator which can be activated to control gene expression (31). GBS encodes approximately 21 unique TCS, which is more than other Streptococcal species such as *Streptococcus pneumoniae* and *Streptococcus pyogenes*, suggesting the importance of these regulators in this opportunistic pathogen (32, 33). Perhaps the most well-studies TCS in GBS is CovRS, encoding a sensor histidine kinase (*covS*) and a response regulator (*covR*). CovR represses the expression of multiple GBS virulence factors including fibrinogen and plasminogen binding proteins and the β-hemolysin (34). CovR regulation has been shown to be important for GBS vaginal colonization and development of invasive disease (35, 36).

Here, we describe for the first time the development of a murine model of GBS diabetic wound infection to begin to assess host-pathogen interactions in this environment. We find that GBS infection in the diabetic wound promotes a hyper-inflammatory response with increased cytokine production and neutrophil degranulation. GBS responds to the inflammatory environment with the upregulation of numerous virulence factors such as *pbsP* and *cylE*, which are necessary for full GBS virulence in diabetic infection and acquiring mutations in *covR* during diabetic wound infection. Taken together, these results present numerous strategies by which GBS adapts to the hyper-inflammatory diabetic wound environment and provides insight into the pathogenic mechanisms of GBS diabetic wound infection.

Results

Development of a Murine Model of GBS Diabetic Wound Infection.

We developed a murine model of GBS diabetic wound infection using *Lepr*^{db} mice. These mice harbor a mutation in the leptin receptor gene which results in obesity and mimics type 2 diabetes (37, 38). Mice were wounded with a 6 mm biopsy punch on their backs, infected with 1 x 10^7 CFU of GBS and wrapped with an adhesive to allow efficient bacterial inoculation. Once the adhesive was removed, and animals were left for additional time before sacrifice, tissue collection and bacterial enumeration (**Fig 1A**). All mice exhibited non-fasting glucose levels above 250 mg/dL to be considered diabetic and levels under 200 mg/dL for non-diabetic controls (**Fig 1B**). Following GBS infection, diabetic animals had significantly larger wounds at the time of sacrifice than WT C57Bl/6 controls with the average wound size of non-diabetic mice being 47 mm and diabetic being 1.16 mm (p-value= .0485, standard deviations .254 and .429 respectively) (**Fig 1C,D**). In addition, we utilized three clinically relevant GBS strains representing the three of the five most prominent serotypes associated with disease worldwide; A909 (serotype Ia), COH1 (serotype III) and CJB111 (serotype V) (30). Regardless of strain, we found that even at an early time point of infection there were significantly more bacteria recovered from the wounds of diabetic animals in comparison to the non-diabetic (**Fig 1E**). These data support clinical findings that GBS persists in the diabetic wound environment (19, 39), and provide a relevant model for further investigation.

Further, we obtained 27 clinical isolates of GBS recovered from diabetic wounds of human patients, and determined the molecular serotype of each isolate using primers specific to *cps* loci (40). Serotypes Ia, Ib, II and III were confirmed by flow cytometry as described by Burcham et al. using monoclonal antibodies against capsule (41). The most prominent serotype

was Ia, which represented one third of all isolates recovered (**Table 1**). The remaining isolates were serotype V (22.22%), II (22.22%), III (11.11%) and Ib (7.41%) with one isolate that was unable to be typed by either PCR or flow cytometry (**Table 1**).

Diabetic animals upregulate inflammatory pathways and immune cell recruitment upon GBS infection.

To determine the host response upon wound infection with GBS, we performed dual RNA-sequencing of both diabetic and non-diabetic animals in comparison to animals inoculated with a PBS control. Principal component analysis (PCA) plots demonstrate that diabetic and non-diabetic animals clustered more similarly with infected vs. uninfected animals also clustering closely (**Fig 2A**). Analysis of the host response in diabetic vs non-diabetic animals that were inoculated with PBS revealed upregulation of genes involving epithelial mesenchymal transition, interferon alpha response, inflammation and adipogenesis (**Supplementary Fig 1**). These data support current literature on the improper immune response associated with diabetes and hyper-inflammation of diabetic wounds (1, 42, 43).

We next sought to determine how infection with GBS affected gene expression in diabetic mice. When comparing the transcriptome of diabetic animals infected with GBS compared to PBS controls, 199 transcripts were significantly upregulated (Log2 fold-change > 2, p-value< .05) with some of the most highly upregulated transcripts including the subunits of calprotectin (s1008a and s100a9), myeloperoxidase (*mpo*) and elastase (*elane*) (**Fig 2B**). We utilized Reactome pathway analysis as well as gene set enrichment analysis (GSEA) to link upregulated genes to known cellular pathways (44). Significantly upregulated pathways in GSEA

included interferon gamma response, TNF alpha signaling via NFkB, complement, inflammatory response and reactive oxygen species (**Fig 2C**). NFkB activation has been linked to an amplified inflammatory state in chronic wounds due to increased production of inflammatory cytokines (7). Some of the most significant pathways up in Reactome analysis were neutrophil degranulation, IL-10 signaling and the formation of a fibrin clot (**Table 2**). A multitude of cytokines and chemokines were upregulated, indicating recruitment of immune cells to the diabetic wound environment (**Table 2**). Finally, some of the most highly upregulated transcripts following GBS infection were proteolytic enzymes including matrix metalloprotease 8, elastase and cathepsin G.

GBS triggers inflammation in diabetic wound tissue.

The upregulation of inflammatory pathways led us to hypothesize that GBS triggers increased inflammation in the diabetic wound. To test this hypothesis, we quantified the levels of inflammatory cytokines and chemokines in addition to neutrophil markers in wound tissue. Mice infected with GBS lost significantly more weight over the course of infection than uninfected controls, and none of the uninfected mice had any GBS recovered from wound tissue (**Fig 3A,B**). H&E staining of wound tissue sections demonstrate a gross difference in tissue architecture from GBS infected mice including thickening of the epithelial layer and inflammatory infiltrate (**Fig 3C**). To confirm this in the wound we used ELISA to determine that GBS infected wounds had significantly greater abundance of the neutrophil chemoattractant KC (homologous to human CXCL1) further supporting that GBS infection triggers the recruitment of neutrophils to the site of infection (**Fig 3D**). Finally, we determined that the abundance of neutrophil components elastase, myeloperoxidase and a subunit of calprotectin are significantly higher during GBS infection (**Fig 3E-G**). Collectively, these data suggest that GBS promotes inflammation in the

already highly inflammatory diabetic wound environment and confirms the upregulation of these pathways and genes observed in our RNA-seq analysis (**Table 2**).

GBS transcriptome in diabetic wound infection.

To characterize the bacterial response in the diabetic wound environment, we performed RNA-sequencing on GBS isolated from non-diabetic and diabetic wounds in comparison to GBS grown *in vitro* (input control). PCA plots indicate that each group clusters independently, with the largest variation being between the input control bacteria and the bacteria isolated from the mice (**Fig 4A**). A total of 979 transcripts were significantly altered (minimum fold change of 3, p-value <.05) when comparing GBS isolated from diabetic infection in comparison to the input control with 462 being upregulated (**Fig 4B**). Further analysis of genes dysregulated during diabetic infection revealed multiple housekeeping genes were downregulated during GBS infection including ribosomal subunit genes *rpsC*, *rpsV* and *rpsE*. (**Fig 4C**) and numerous virulence associated genes were upregulated in comparison to the input control (**Fig 4C**, **Table 3**). Some of the most highly upregulated transcripts in diabetic infection include the gene encoding the surface plasminogen binding protein PbsP, the *cyl* operon encoding GBS hemolysin and pigment, quorum sensing peptide pheromone *shp2*, nuclease and protease encoding genes such as *nucA* and *clpL*, as well as various predicted effectors of the type VII secretion system (**Table 2**). Interestingly, many of these factors are known to be part of the core regulon of the CovRS TCS (45–47).

The CovRS regulon contributes to diabetic wound infection.

We observed when plating GBS recovered from the diabetic wound that many colonies were hyperpigmented, with some experiments having hyper-pigmented colonies recovered from

up to 83.3% of all diabetic mice (**Fig 5A**). These phenotypes were stable, and colonies were hyperhemolytic when plated on sheep's blood agar (**Fig 5B**). Notably, we have never recovered a hyper-pigmented colony from a non-diabetic mouse. Hyperpigmentation and hyper-hemolysis in numerous GBS strains has been attributed to mutations in the *covRS* TCS, due to the subsequent de-repression of the *cyl* operon which is linked to GBS hemolysis and pigment production (25, 48–52). We surveyed the *covR* locus from hyperpigmented/ hyperhemolytic strains recovered from 13 different mice for single nucleotide polymorphisms (SNPs) and observed multiple SNPs resulting in mutations in the *covR* locus (**Table 4**. Of these mutations, 8/13 encoded for amino acid substitutions in the receiver domain of CovR and would likely disrupt the CovR dimerization domain (**Fig 5C**). Nonpigmented colonies were also isolated and sequenced from each mouse containing a hyperpigmented colony and none of the nonpigmented colonies had mutations in *covR*. We hypothesized due to the upregulation of the *cyl* operon in diabetic wound infection and the spontaneous *covR* mutations *in vivo*, that a *ΔcylE* mutant would be attenuated in diabetic wound infection. In confirmation, we infected diabetic mice with the *ΔcylE* mutant strain and observed a significant decrease in bacteria recovered from wound tissue compared to WT infected mice (**Fig 5D**). Further, wounds from *cylE* infected mice had a significant reduction in the abundance of the chemokine KC (CXCL1) (**Fig 5E**).

The surface protein PbsP contributes to diabetic wound formation via adherence to the skin.

The most highly upregulated gene during GBS diabetic wound infection encodes the surface plasminogen binding protein PbsP (**Table 3**). Interestingly, *pbsP* has been shown to be repressed by CovR in multiple GBS strains (26, 34, 53). In addition, PbsP is known to bind multiple extracellular matrix components such as plasminogen and fibrinogen (26) and

contribute to adherence to colon epithelial and brain endothelial cells (26, 54, 55) We therefore hypothesized that PbsP contributes to diabetic wound infection via adherence to the skin. A *pbsP* mutant is significantly attenuated in diabetic wound infection in comparison to WT (**Fig 6A**). Further, *pbsP* mutant infected tissues have significantly less abundance of neutrophil markers MPO, elastase and calprotectin, which are all upregulated during GBS diabetic wound infection (**Table 2**) (**Fig 6B-D**). We next tested the ability of the *pbsP* mutant to adhere to skin cells *in vitro*. Using a cell culture line of immortalized keratinocytes (NTERTs), we found that a *pbsP* mutant had a ~50% reduction in adherence to skin epithelial cells that could be restored by complementing the mutant with WT *pbsP* (**Fig. 6E**) (56). These data suggest that PbsP contributes to diabetic wound infection and direct interaction with skin keratinocytes.

Discussion

A hallmark characteristic of diabetic individuals is an altered neutrophil response due to persistent hyperglycemia. Neutrophils from diabetic individuals are often pro-inflammatory, exhibiting increased neutrophil extracellular trap (NET) formation, pro-inflammatory cytokine production and extracellular ROS generation (1, 57). Additionally, decreased apoptosis, neutrophil migration and intracellular ROS production have been shown in diabetic individuals, leading to impaired bacterial killing (58). Persistent inflammation and decreased bacterial clearance are detrimental to diabetic individuals who develop wounds, as resolution of inflammation is paramount to proper wound healing (59). GBS is one of the most commonly isolated pathogens from diabetic wounds, and has been shown to promote inflammation and neutrophil influx during lung infection as well as during sepsis (11, 50, 60). Here, we have utilized dual RNA-sequencing to determine the transcriptional consequences of GBS infection of diabetic wounds on both the host and pathogen. We demonstrate that GBS exacerbates inflammation in the already hyper-inflammatory diabetic wound environment and identify the first mechanisms by which GBS adapts to this hyper-inflammation. The data herein are the first to provide insight into GBS pathogenesis in this clinically relevant model of infection.

We demonstrate that GBS burden is significantly greater in diabetic wounds than non-diabetic, and that these data remain consistent regardless of GBS capsular serotype. GBS infection of diabetic wounds resulted in significant upregulation of pathways involved in the inflammatory response and ROS production in comparison to diabetic wounds without GBS. These findings are particularly interesting as diabetic animals already exhibit significant upregulation of these pathways in comparison to non-diabetic controls, suggesting that the presence of GBS exacerbates inflammation during diabetes. We speculate that GBS promotes

inflammation as a strategy to stall wound healing and closure. The presence of microbes has been linked to neutrophil influx in chronic wounds, but studies on specific bacterial factors that assist in promoting and surviving inflammation are limited.

Our bacterial RNA-sequencing revealed that GBS upregulates numerous virulence factors during diabetic wound infection in comparison to those grown in laboratory media. The most highly upregulated GBS gene in diabetic wound infection encodes for the surface plasminogen binding protein PbsP, which binds to extracellular matrix components such as plasminogen and fibrinogen (26). Plasminogen binding proteins are known to bind plasminogen, and, in the presence of a tissue activator, activate plasminogen into plasmin (61). While plasminogen is crucial in early wound healing to promote inflammation, it's resolution is necessary to progress tissue healing into the proliferation phase (62, 63). A Δ*pbsP* mutant is attenuated in multiple GBS models of infection including in vaginal colonization and meningitis (54, 64). Furthermore, Lentini et al. demonstrated that brain tissue homogenates from mice infected with a Δ*pbsP* mutant had a significant reduction in MPO, TNFα and IL-1β abundance in comparison to WT infected mice (54). Here, we demonstrate that PbsP is required for GBS diabetic wound infection, and that Δ*pbsP* mutant infected wounds have significantly less MPO, elastase and calprotectin than those infected with WT. We hypothesize that PbsP binding to host plasminogen is necessary for GBS mediated inflammation via increased cytokine and chemokine signaling as well as increased plasmin production that degrades host matrix components necessary for proliferation and remodeling of the skin. Further work on the exact mechanism of PbsP mediated inflammation is being elucidated.

We next investigated the GBS hemolysin/ pigment encoded by the *cyl* operon, which was also highly upregulated during diabetic infection. Studies on the *cylE* component of this operon

have shown that CylE contributes to GBS pathogenesis in murine models of sepsis and lung infection, and that induction of the neutrophil chemoattractant IL-8 was significantly reduced in A549 cells infected with a *cylE* mutant (50, 51). Diabetic wounds from mice infected with a *ΔcylE* mutant had significantly fewer bacteria recovered than those infected with WT GBS, coupled with significantly less abundance of the neutrophil chemoattractant KC (CXCL1). CXCL1 is known to attract neutrophils to the site of infection, and the abundance of CXCL1 in chronic wounds is high in comparison to burn or surgical wounds (65). We therefore hypothesize that production of the GBS hemolysin/pigment is necessary for GBS to trigger neutrophil influx into the diabetic wound environment.

Other factors that were highly upregulated during diabetic wound infection included the nuclease *nucA*, and the quorum sensing (QS) genes *shp2* and *rovS*. NucA is the major GBS nuclease and has been shown to degrade NETs as well as contribute to virulence in the lung (66). We speculate that the upregulation of *nucA* might be in response to the hyper-inflammatory environment, and in particular, the increased NET production which is associated with diabetic wounds (1, 57). Increased nuclease activity could therefore assist GBS in evading NETs and persisting in the diabetic wound environment, although further experiments are warrented to determine this. Increased production of *shp2* and *rovS* suggests a need for bacterial cell-to-cell communication in the diabetic wound environment. The need for QS systems in wounds is well-documented in both *S. aureus* and *P. aeruginosa*, which both rely on QS systems for full virulence and persistence in chronic wounds (67, 68). While GBS *shp2* and *rovS* are required for GBS to persist in the murine liver and spleen (69), no work has investigated whether this QS system is critical to survival in the wound environment. Additionally, GBS *shp2* and *rovS* have a

known role in interspecies communication which could highlight the importance of these genes in a polymicrobial diabetic wound environment (70).

In addition to our findings that GBS promotes hyper-inflammation in diabetic wounds via both the surface protein PbsP and CylE, we noticed that GBS colonies recovered from diabetic wounds were often hyperpigmented and encoded mutations in the TCS *covRS*. CovR represses numerous GBS virulence factors including the *cyl* operon as well as *pbsP* in multiple GBS strains (25, 35, 46). Of note, is that spontaneous mutations in the *covRS* locus of GBS have been identified in clinical isolates from patients with necrotizing fasciitis, sore throat, and prosthetic joint infection (48, 49, 71). In addition, numerous studies of *Streptococcus pyogenes* (GAS) have linked spontaneous mutations in *covRS* to invasive infection in this pathogen (72, 73). Interestingly, we have not recovered any hyper-pigmented colonies from non-diabetic animals. We therefore speculate that the diabetic environment is promoting the selection of *covR* mutants in the wound. This selection would result in increased expression of GBS virulence factors that could promote survival in this niche. The exact environmental factors that may promote *covR* mutations in the diabetic wound are currently unknown.

The work presented herein establishes the first murine model of GBS diabetic wound infection. Using our model, we define changes in both the host and pathogen transcriptome in the murine diabetic wound environment and demonstrate that GBS promotes inflammation which contributes to the chronic wound environment. As we demonstrate, this model is an efficient tool to investigate GBS pathogenesis, and potentially other pathogens, in the context of diabetic wounds. Our results emphasize the importance of further studies on GBS pathogenesis and the innate immune response at the diabetic wound interface.

Acknowledgments

We would like to thank Elizabeth Grice and Sue Gardner for providing clinical GBS isolates, Laura Cook for providing the Δ*pbsP* mutant, and Amber Nguyen for assistance with sequencing. This work was supported by NIH grants R01NS116716, R01AI153332 to K.S.D., NIHT32DK120521 to R.A.K. and R01AI153185 to A.R.H., and Department of Veteran Affairs Award BX002711 to A.R.H.

Figures, tables and legends

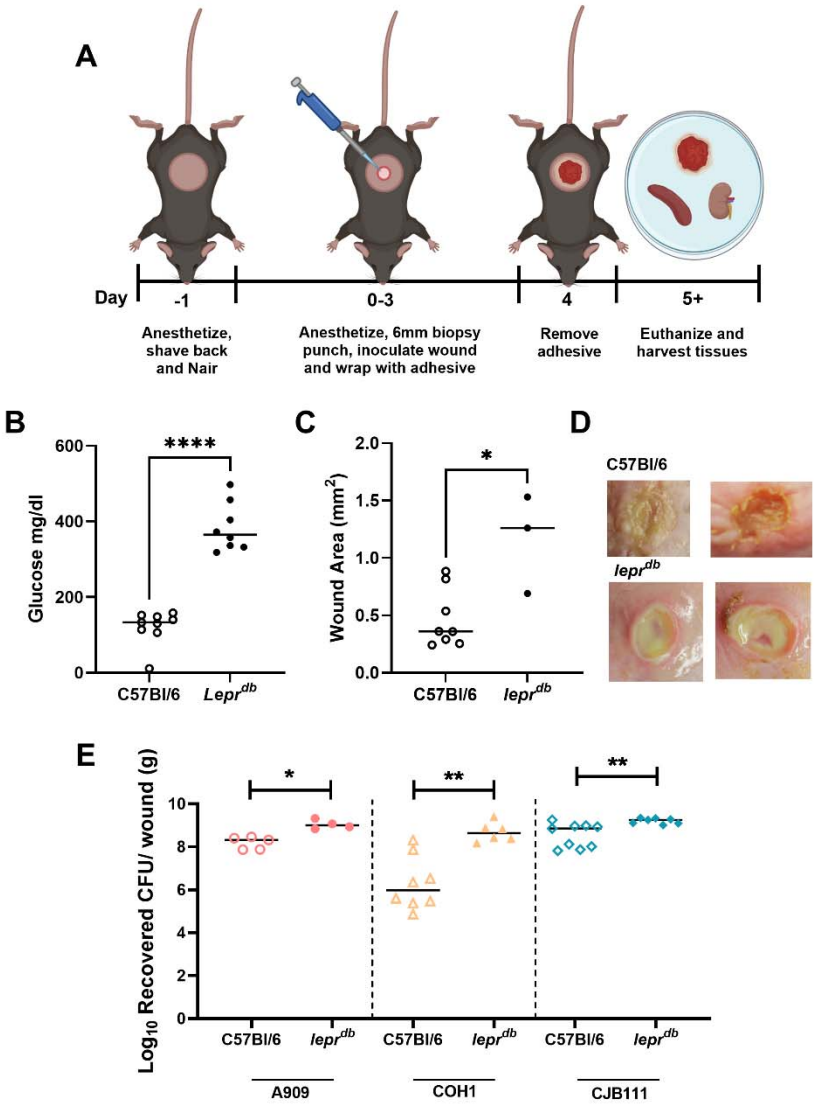

Figure 1. Murine Model of GBS Diabetic Wound Infection. (A) Schematic of the murine model of diabetic wound infection. (B) Non-fasting glucose levels from the blood of mice the day of infection. (C) Wound area calculated in ImageJ from representative mice following GBS infection. (D) Representative images of GBS infected wounds from non-diabetic and diabetic mice on the day of sacrifice. (E) CFU recovered from wounds of non-diabetic and diabetic mice

after GBS infection. Significance determined by Mann–Whitney U test; *p<.05, **p<.01, ****p<.0001.

Serotype	Ia	Ib	II	III	V	Undetermined
Distribution	9/27 (33.33%)	2/27 (7.41%)	6/27 (22.22%)	3/27 (11.11%)	6/27 (22.22%)	1/27 (3.7%)
Strain numbers	112[C]	503[I]	69[C]	64[C]	98[C]	734[I]
	836[I]	1418[I]	85[C]	113[C]	103[C]	
	884[I]		157[C]	361[I]	130[C]	
	982[I]		330[I]		809[I]	
	1052[I]		607[I]		914[I]	
	1394[I]		1962[I]		1101[I]	
	1463[I]					
	1852[I]					
	2000[I]					

Isolates obtained from Colorado are designated with a [C] and isolates from Iowa an [I].

Table 1. Clinical isolate serotypes.

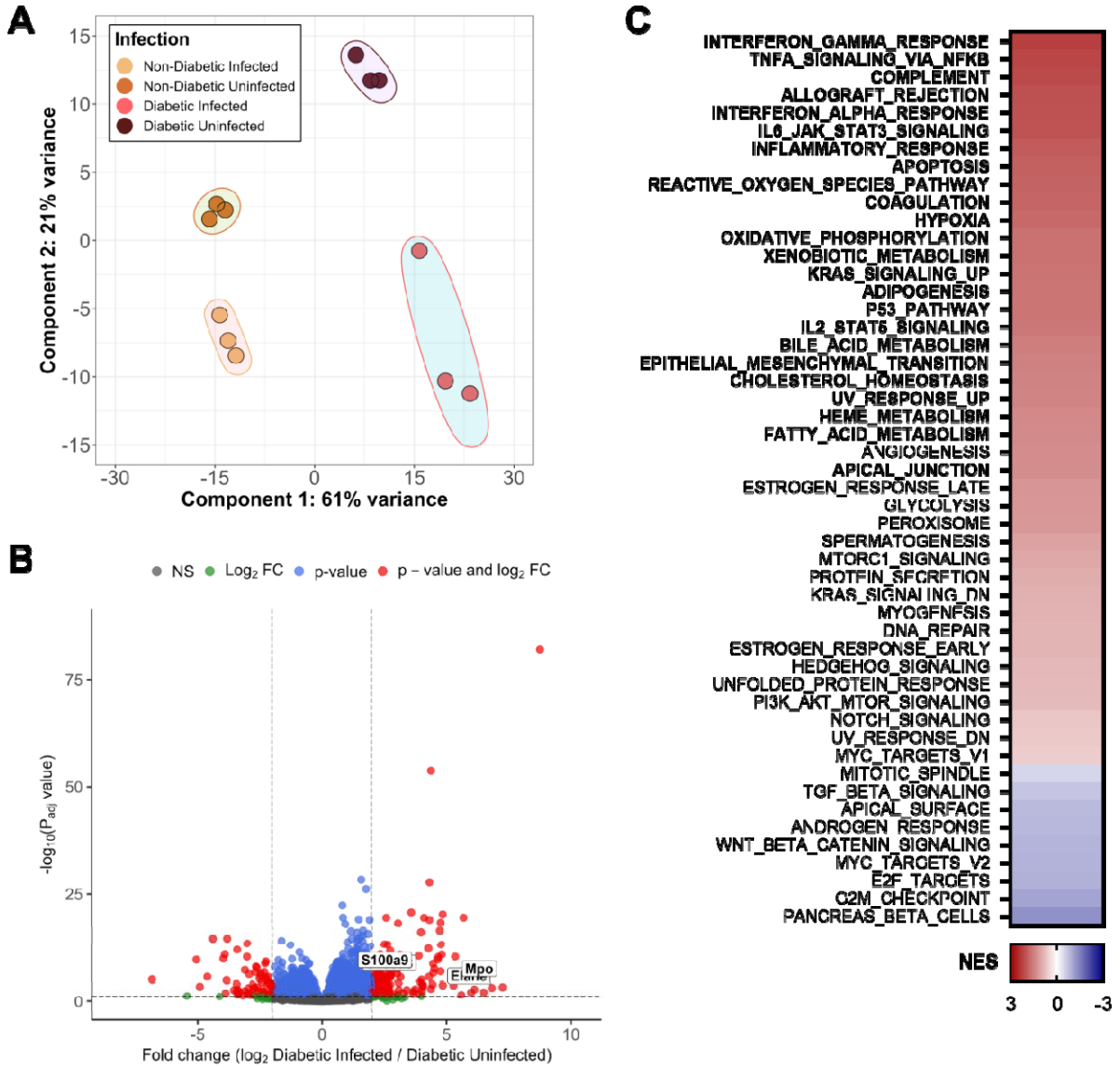

Figure 2. Diabetic animals upregulate inflammatory pathways and immune cell recruitment upon GBS infection. (A) PCA plot of murine transcriptome from RNA-seq analysis. (B) Gene set enrichment analysis of diabetic animals infected with GBS vs. uninfected controls. Significant pathways in bold. (C) Volcano plot for differentially expressed genes when comparing diabetic mice infected with GBS to uninfected controls.

Gene ID	DAVID Description	Fold change
Formation of a Fibrin Clot		
Fga	fibrinogen alpha chain(Fga)	69.55
Kng1	kininogen 1(Kng1)	32.90
Fgg	fibrinogen gamma chain(Fgg)	16.34
Cd177	CD177 antigen(Cd177)	15.03
Prtn3	proteinase 3(Prtn3)	6.82
Gp9	glycoprotein 9 (platelet)(Gp9)	4.35
Neutrophil degranulation		
Ms4a3	membrane-spanning 4-domains, subfamily A, member 3(Ms4a3)	152.22
Mpo	myeloperoxidase(Mpo)	81.57
Elane	elastase, neutrophil expressed(Elane)	60.97
Camp	cathelicidin antimicrobial peptide(Camp)	52.71
Mmp8	matrix metallopeptidase 8(Mmp8)	26.54
Prg2	proteoglycan 2, bone marrow(Prg2)	22.63
Lcn2	lipocalin 2(Lcn2)	21.26
Epx	eosinophil peroxidase(Epx)	20.68
Abca13	ATP-binding cassette, sub-family A (ABC1), member 13(Abca13)	20.39
Pglyrp1	peptidoglycan recognition protein 1(Pglyrp1)	15.78
Cd177	CD177 antigen(Cd177)	15.03
Itgam	integrin alpha M(Itgam)	13.27
Mgam	maltase-glucoamylase(Mgam)	9.58
Mmp25	matrix metallopeptidase 25(Mmp25)	8.88
Ctsg	cathepsin G(Ctsg)	8.46
Olfm4	olfactomedin 4(Olfm4)	8.22
Fpr1	formyl peptide receptor 1(Fpr1)	6.92
Prtn3	proteinase 3(Prtn3)	6.82
S100a8	S100 calcium binding protein A8 (calgranulin A)(S100a8)	6.63
Gpr84	G protein-coupled receptor 84(Gpr84)	6.50
Serpinb3d	serine (or cysteine) peptidase inhibitor, clade B (ovalbumin), member 3D(Serpinb3d)	6.11
S100a9	S100 calcium binding protein A9 (calgranulin B)(S100a9)	5.86
Serpina3g	serine (or cysteine) peptidase inhibitor, clade A, member 3G(Serpina3g)	5.70
Cxcr1	chemokine (C-X-C motif) receptor 1(Cxcr1)	5.35
Gzmb	granzyme B(Gzmb)	5.03
Tarm1	T cell-interacting, activating receptor on myeloid cells 1(Tarm1)	4.89
Cxcl1	chemokine (C-X-C motif) ligand 1(Cxcl1)	4.59
Ear1	eosinophil-associated, ribonuclease A family, member 1(Ear1)	4.50
Slco4c1	solute carrier organic anion transporter family, member 4C1(Slco4c1)	4.14
Signaling by Interleukins		
Nos2	nitric oxide synthase 2, inducible(Nos2)	25.81
Lcn2	lipocalin 2(Lcn2)	21.26
Itgam	integrin alpha M(Itgam)	13.27
Saa1	serum amyloid A 1(Saa1)	12.21
Ccl5	chemokine (C-C motif) ligand 5(Ccl5)	9.78
Ifng	interferon gamma(Ifng)	8.51
Ctsg	cathepsin G(Ctsg)	8.46
Csf2	colony stimulating factor 2 (granulocyte-macrophage)(Csf2)	8.22
Fpr1	formyl peptide receptor 1(Fpr1)	6.92
Il27	interleukin 27(Il27)	6.82
Prtn3	proteinase 3(Prtn3)	6.82
Il12a	interleukin 12a(Il12a)	6.41
Ebi3	Epstein-Barr virus induced gene 3(Ebi3)	5.98
Il12b	interleukin 12b(Il12b)	5.66
Gzmb	granzyme B(Gzmb)	5.03
Cxcl1	chemokine (C-X-C motif) ligand 1(Cxcl1)	4.59

Table 2. Select pathways and genes enriched upon GBS infection of diabetic wounds.

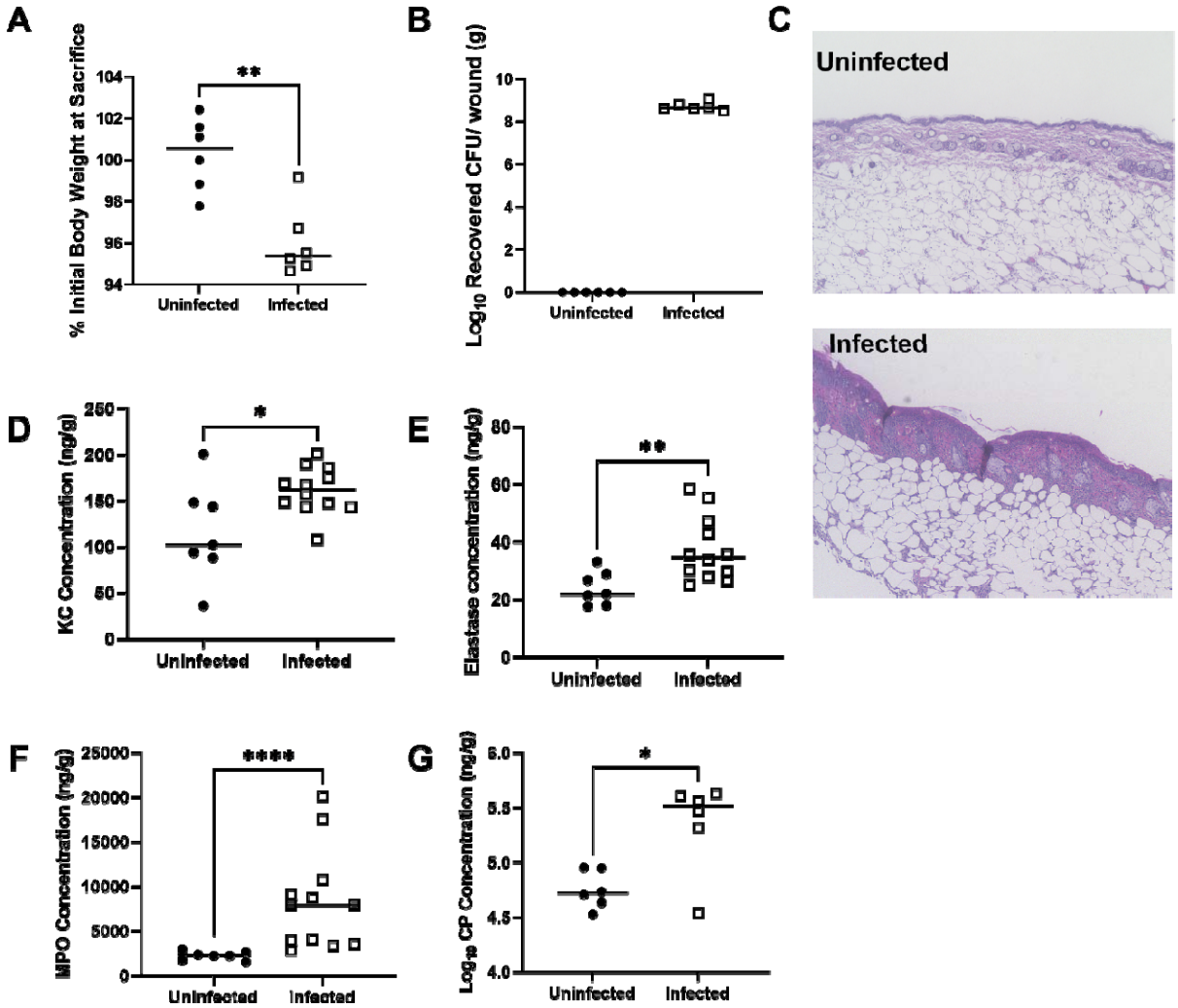

Figure 3. GBS triggers inflammation in diabetic wound tissue. (A) Percent initial body weight of mice after GBS infection. (B) GBS recovery from wound tissues of uninfected vs. infected mice. (C) Histology of diabetic wound tissue at time of sacrifice. Scale bars set to 10 µm (need to put in). (D-G) ELISAs on tissue homogenates at time of sacrifice. All concentrations were normalized to tissue weight. Significance determined by Mann-Whitney U-test; *p<.05, **p<.01, ****p<.0001.

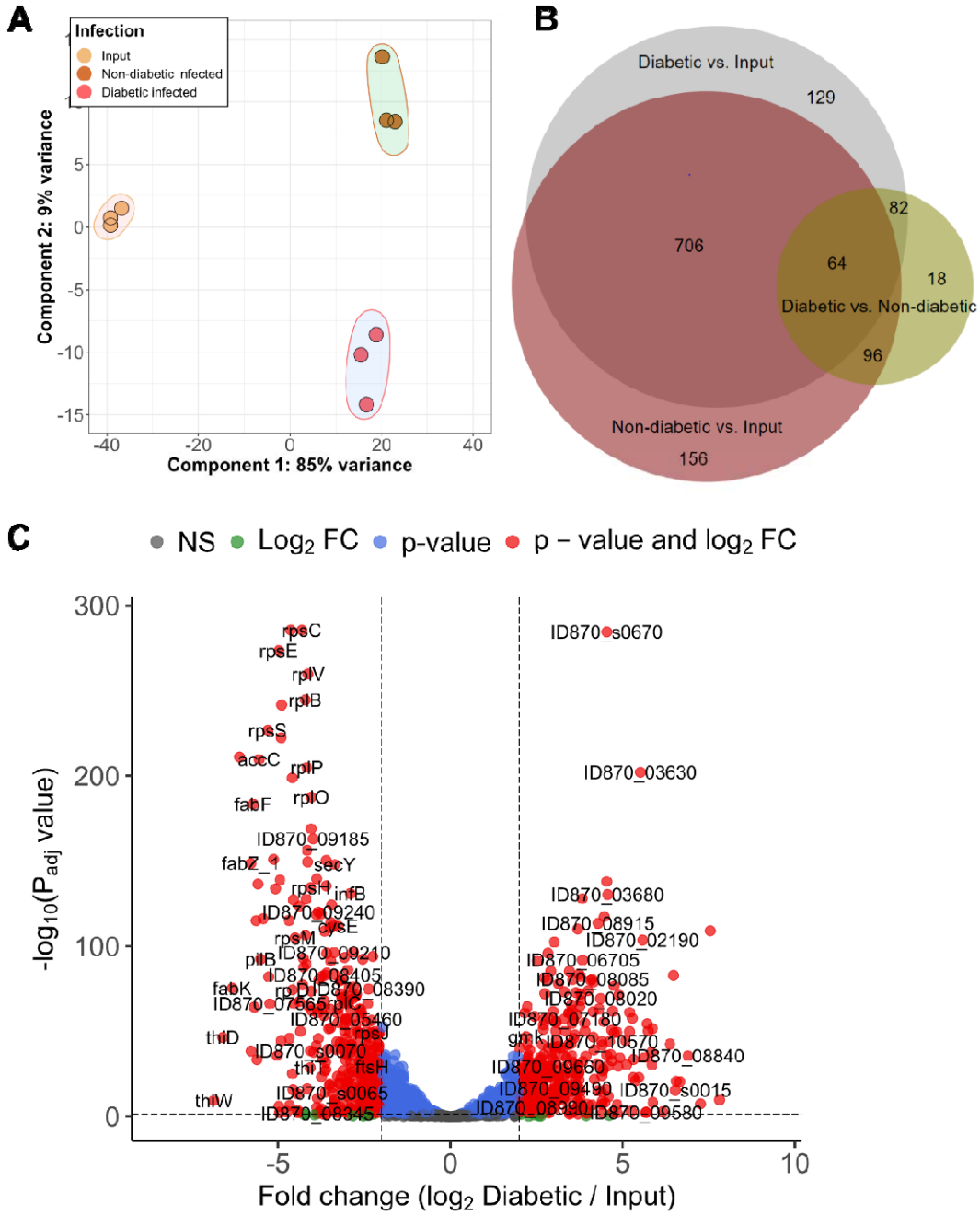

Figure 4. GBS upregulates the surface protein PbsP in wound infection. (A) PCA plot of bacterial transcriptome in RNA-seq. (B) Venn diagram of differentially expressed genes in each comparison. (C) Volcano plot of differentially expressed genes in diabetic infection vs. input.

Gene number (CJB111 genome)	Gene name	Description	Diabetic v. Input
ID870_07365	*pbsP*	YSIRK signal domain/LPXTG anchor domain surface protein	186.61
ID870_02195	*shp2*	peptide pheromone SHP2	101.66
ID870_05830	*nucA*	DNA/RNA non-specific endonuclease	83.14
ID870_02190		transglutaminase, regulated by shp2 RovS	47.73
ID870_03115	*clpL*	ATP-dependent Clp protease ATP-binding subunit	26.96
ID870_07100		type II toxin-antitoxin system RelB/DinJ family antitoxin	25.86
ID870_07095		toxin-antitoxin system, toxin component, MazF family protein	23.11
ID870_10045		alpha/beta hydrolase	22.10
ID870_03740	*tpx*	thiol peroxidase	15.03
ID870_03230		Ltp family lipoprotein	13.85
ID870_08245		WXG100 family type VII secretion target	13.12
ID870_04175		WXG100 family type VII secretion target	11.10
ID870_06190		type II toxin-antitoxin system death-on-curing family toxin	9.97
ID870_04170		WXG100 family type VII secretion target	8.94
ID870_05905	*cylK*	CylK protein	8.91
ID870_08300		type II toxin-antitoxin system RelE/ParE family toxin	8.53
ID870_02285		LPXTG cell wall anchor domain-containing protein	8.48
ID870_06195		type II toxin-antitoxin system Phd/YefM family antitoxin	8.36
ID870_01270		Asp23/Gls24 family envelope stress response protein	8.20
ID870_10470	*cfb*	CAMP factor pore-forming toxin Cfb	7.82
ID870_10565		WXG100 family type VII secretion target	5.93
ID870_03660		CidA/LrgA family protein	5.05
ID870_00915		3'-5' exonuclease	4.79
ID870_05925	*cylE*	cylE protein	3.85
ID870_05955	*cylD*	CylD	3.82
ID870_00425		glycoside hydrolase family 88 protein	3.80
ID870_05890		S8 family serine peptidase	3.44
ID870_03865		lipase	3.34
ID870_05910	*cylJ*	cylJ protein	2.71
ID870_04105	*fbsA*	fibrinogen-binding adhesin FbsA	2.67
ID870_05960	*cylX*	cylX protein	2.60
ID870_05645		Cof-type HAD-IIB family hydrolase	2.44
ID870_07205		S8 family serine peptidase	2.26

Table 3. GBS Virulence factors upregulated in diabetic infection vs. input control.

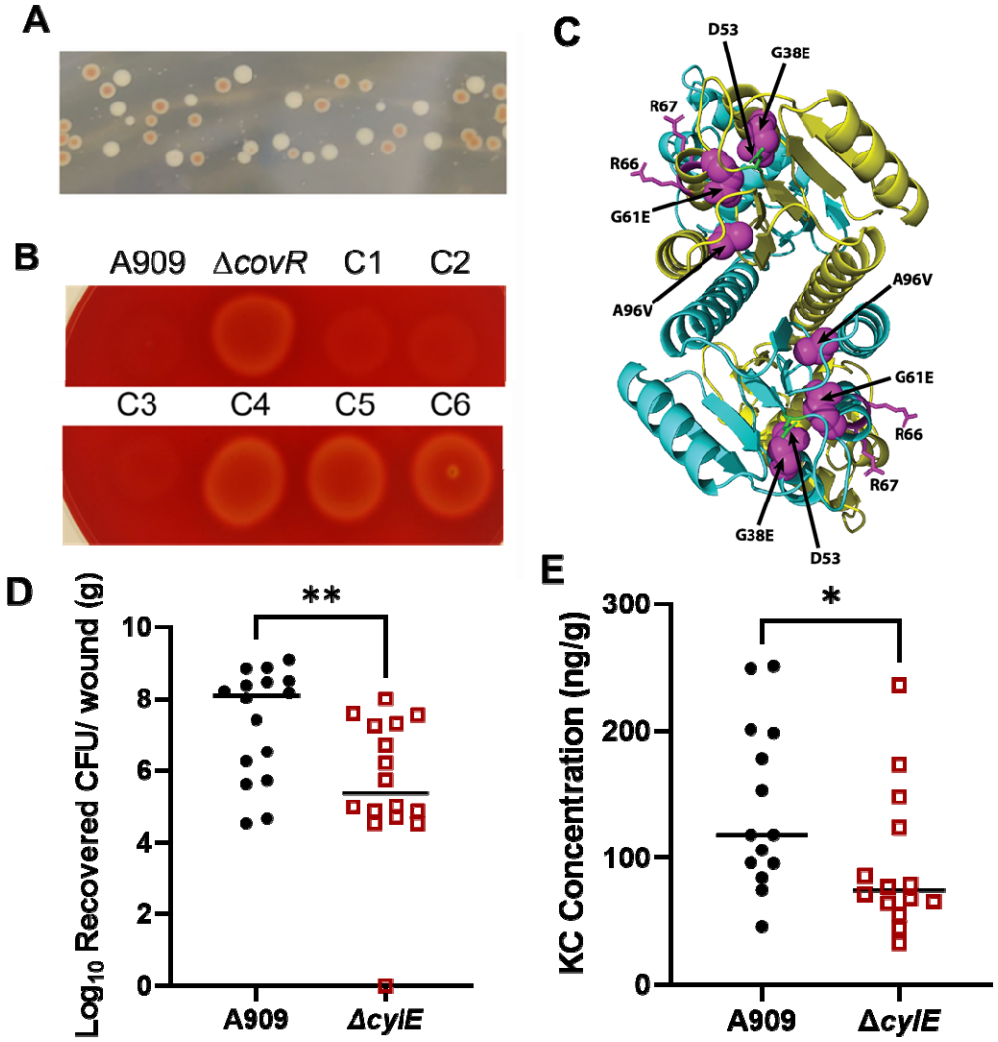

Figure 5. The CovRS Regulon Contributes to Diabetic Wound Infection. (A) GBS colonies on THA recovered from diabetic wounds. (B) Hyperpigmented colonies plated on sheep's blood agar; C1-3 from non-pigmented colonies and C4-6 from pigmented colonies (C) Structural model of CovR mutations on VanR structure from *Streptomyces coelicolor*. (D) CFU of GBS recovered from diabetic wound tissue. (E) KC concentration recovered from wound tissue homogenates. All ELISA data is normalized to tissue weight. Significance determined via Mann Whitney U-test; *p<.05, **p<.01.

Category	AA Position	Nucleotide position	Substitution
AA Substitution	G38		Gly-to-Glu
	A96		Ala-to-Val
	R66		Arg-to-Cys
	G61		Gly-to-Asp
	D53		Asp-to-His
	R67		Arg-to-Pro
	R67		Arg-to-Cys
	A96		Ala-to-Val
Nucleotide deletion		387	Deletion of A
		169	Deletion of T
	V31		Deletion of Val
Insertion/deletion		123	Multiple nucleotides deleted
		35	Multiple nucleotides inserted

Table 4. Mutations in *covR* from hyperpigmented colonies recovered from the diabetic wound.

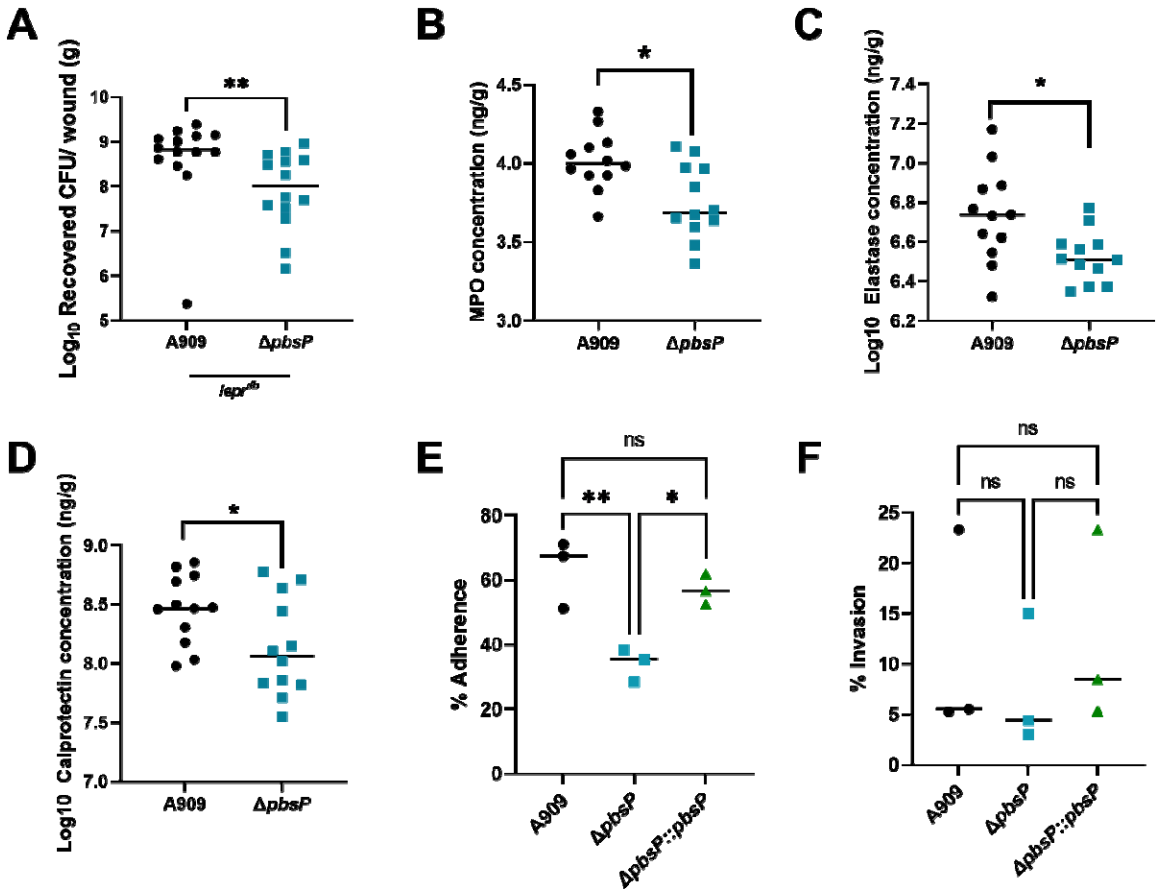

Figure 6. PbsP contributes to GBS burden and inflammation in the diabetic wound. (A) CFU recovered from diabetic mice infected with A909 or a Δ*pbsP* mutant. (B,C,D) MPO, Elastase, and Calprotectin concentration recovered from wound tissue homogenates. All ELISA data is normalized to tissue weight. (E) GBS adherence to immortalized keratinocytes with either wildtype, mutant or complemented PbsP. Significance determined via Mann Whitney U-test; *p<.05, **p<.01.

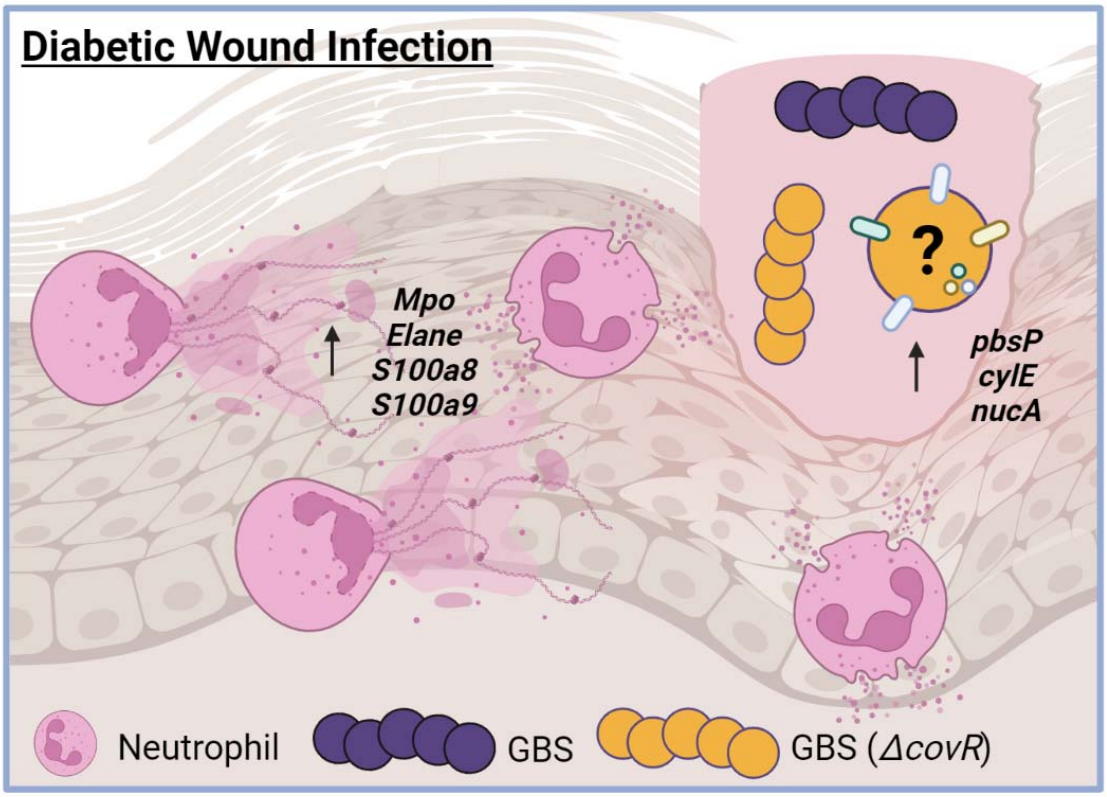

Figure 7. Model for GBS pathogenesis in the diabetic wound. Image generated in BioRender.

388

389

Materials and Methods

Bacterial strains and growth conditions. GBS strains A909, COH1 and CJB111 were used in this study. GBS strains were grown in Todd Hewitt Broth (THB; Research Products International, RPI) statically at 37˚ C. When needed, antibiotic was added to THB at final concentrations of 100 μg/mL spectinomycin. Strains containing the plasmid pDCErm were grown in THB + 5 μg/mL erythromycin. All strains used in this study can be found in **Table S1** and primers in **Table S2.** The human immortalized keratinocyte cell line N/TERT-2G cells were kindly gifted from Dr. Johann Gudjonsson with permission from Dr. Jim Rheinwald and were maintained up to 25 passages at 37 ˚C with 5% CO_2 according to methods described in Dickson et al., 2000 (56).

Ethics statement. Animal experiments were approved by the Institutional Animal Care and Use Committee (IACUC) at University of Colorado Anschutz Medical Campus protocol #00987 and were per- formed using accepted veterinary standards. The University of Colorado Anschutz Medical Campus is AAALAC accredited; and its facilities meet and adhere to the standards in the "Guide for the Care and Use of Laboratory Animals".

Murine model of wound infection. Female, 8-week-old C57Bl/6 mice or *Lepr*^{db} mice were anesthetized with isoflurane the day prior to infection. The backs of the mice were shaved and treated with Nair and tail snips were performed to measure blood glucose levels with a glucometer. The next day mice were weighed and again anesthetized before undergoing wounding procedure. The backs of mice were disinfected with iodine wipes and then wounded with a 6 mm biopsy punch. Following, 1 x 10^7 CFU of GBS or PBS control was added before wrapping the mice in the adhesive Tegaderm™. Wounds were left for 72 h before removal of the adhesive. After another 24 h, mice were sacrificed via CO_2 inhalation and tissues were removed

and homogenized for bacterial enumeration. Tissue homogenates were plated on GBS CHROMagar [SB282(B)], which allows only for the growth of GBS (in pink) and *Enterococcus* spp. (in blue). These experiments were approved by the committee on the use and care of animals at the University of Colorado-Anschutz Medical Campus in our protocol #00987.

Histology. Mice were wounded as described above. Following sacrifice, half of the wound tissue was removed and fixed in formalin for 48 h. After, formalin was removed and wounds were placed into 70% EtOH and sent to the histology core for processing at the Gates Center for Regenerative Medicine, Dermatology at CU Anschutz. Images were taken with a BZ-X710 microscope (Keyence).

RNA preparation and RNA-sequencing. Mice were wounded as previously described and tissue homogenates were used for RNA preparation with the Qiagen RNeasy kit. For mouse samples, RNA was extracted from 2-3 mice before pooling RNA to form triplicate samples. For bacteria, we utilized three input controls as replicates and again pooled from 2-3 mice for all bacterial samples. RNA samples were sent for dual RNA-sequencing (or bacterial RNA-sequencing for input controls), to the Microbial Genome Sequencing Center for Illumina Sequencing and rRNA depletion. Samples were rRNA depleted using RiboZero Plus (Illumina) and libraries for the 12 mouse samples and 3 input bacteria cDNA samples were sequenced using the Illumina Stranded RNA sequencing platform. Raw sequencing reads in fastq format were aligned and annotated to the mouse reference genome (mm10) using Qiagen CLC Genomics Workbench default settings (version 21.0.5): mismatch cost, 2; insertion and deletion cost, 3; length and similarity fraction, 0.8. This process was similarly don’t to identify bacterial transcripts by aligning raw sequencing reads to the Clinical Group B Streptococcal Isolate CJB111 reference genome (CP063198_sRNA) with identical CLC Genomics Workbench settings. Normalization and

differential expression calculations of uniquely mapped mouse or bacterial transcripts were performed using R package DESeq2 (v1.34.0, RRID:SCR_015687) (74). Heatmaps and further comparison of gene expression changes for all mouse and bacterial samples were generated with Rstudio (v1.3.1073, RRID:SCR_000432). Gene set enrichment analysis (GSEA) was performed using the fGSEA R package (v1.20.0, RRID:SCR_020938) with 10,000 permutations and the Hallmarks and GO Biological Processes gene set collections from the Molecular Signatures Database (75).

ELISAs on wound homogenates. Proteins in homogenized tissues was quantified using R&D systems ELISA kits (catalog # DY453, DY667, DY8596-05, DY4517-05). Protein detected was normalized to tissue weight and reported as protein (pg) per mg of tissue.

Adherence of GBS to host cells. Adherence assays were performed as previously described (29, 76). Briefly, cell lines were seeded into 24 well plates and grown to a complete monolayer (approximately 1×10^6 cells/well). GBS was grown to mid-log phase and normalized to 1×10^8 CFU/mL in PBS. 1×10^6 bacteria were added to one well of host cells to achieve a MOI of 1. To assess adherence of GBS to host cells, bacteria were incubated with host cells for 30 min then the cells were washed five times with PBS. Host cells were detached with 0.25% trypsin (Thermo Fisher Scientific) and permeabilized with 0.025% Triton X-100 (Sigma) in PBS, serially diluted, and plated to quantify all cell-associated bacteria.

Statistical analyses. Statistical analysis was performed using Prism version 9.0.0 (121) for Windows (GraphPad Software, La Jolla, CA, United States) as described in figure legends.

Data availability. Mouse and bacterial RNA-sequencing datasets generated in this study were uploaded to NCBI GEO Depository (GSE201342).

Strains used in this study

Strain	Strain type	Antibiotic resistance	Reference
CJB111	Clinical isolate		(77)
A909	Clinical isolate		(78)
COH1	Clinical isolate		(79)
A909 Δ*pbsP*	Mutant	Cm3	(64)
A909 Δ*pbsP::pbsP*	Complement	Cm3, Spec 100	(64)
A909 Δ*cylE*	Mutant	Cm2	(51)

Primers used in this study

Primer Name	Sequence 5' → 3'
Serotype Ia Forward	GGTCAGACTGGATTAATGGTATGC
Serotype Ia Reverse	GTAGAAATAGCCTATATACGTTGAATGC
Serotype Ib Forward	TAAACGAGAATGGAATATCACAAACC
Serotype Ib Reverse	GAATTAACTTCAATCCCTAAACAATATCG
Serotype II Forward	GCTTCAGTAAGTATTGTAAGACGATAG
Serotype II Reverse	TTCTCTAGGAAATCAAATAATTCTATAGGG
Serotype III Forward	TCCGTACTACAACAGACTCATCC
Serotype III Reverse	AGTAACCGTCCATACATTCTATAAGC
Serotype IV Forward	GGTGGTAATCCTAAGAGTGAACTGT
Serotype IV Reverse	CCTCCCCAATTTCGTCCATAATGGT
Serotype V Forward	GAGGCCAATCAGTTGCACGTAA
Serotype V Reverse	AACCTTCTCCTTCACACTAATCCT

References

1. Dowey R, Iqbal A, Heller SR, Sabroe I, Prince LR. 2021. A Bittersweet Response to Infection in Diabetes; Targeting Neutrophils to Modify Inflammation and Improve Host Immunity. Front Immunol 12:1–21.

2. Estelle E, Mathioudakis N. 2018. Update on management of diabetic foot ulcers. Ann N Y Acad Sci 176:139–148.

3. Davidson J. 1995. Wound healing. Adv Dent Res 9:8.

4. Loots MAM, Lamme EN, Zeegelaar J, Mekkes JR, Bos JD, Middelkoop E. 1998. Differences in cellular infiltrate and extracellular matrix of chronic diabetic and venous ulcers versus acute wounds. J Invest Dermatol 111:850–857.

5. Eming SA, Krieg T, Davidson JM. 2007. Inflammation in wound repair: Molecular and cellular mechanisms. J Invest Dermatol 127:514–525.

6. Guest, Christopher B. 2008. The implication of proinflammatory cytokines in type 2 diabetes. Front Biosci Volume:5187.

7. Grice EA, Segre JA. 2012. Interaction of the microbiome with the innate immune response in chronic wounds. Adv Exp Med Biol 946:55–68.

8. Singer AJ, Clark RAF. 1999. Cutaneous Wound Healing. N Engl J Med.

9. Young H, Knepper B, Hernandez W, Shor A, Bruntz M, Berg C, Price CS. 2015. Pseudomonas aeruginosa An Uncommon Cause of Diabetic Foot Infection 105:125–129.

10. Young H, Miller W, Burnham R, Heard S, Berg C, Jenkins TC. How Do Preoperative Antibiotics Affect Culture Yield in Diabetic Foot Infections? 3–6.

11. Kalan LR, Meisel JS, Loesche MA, Horwinski J, Soaita I, Chen X, Uberoi A, Gardner SE, Grice EA. 2019. Strain- and Species-Level Variation in the Microbiome of Diabetic Wounds Is Associated with Clinical Outcomes and Therapeutic Efficacy. Cell Host Microbe 25:641-655.e5.

12. Serra R, Grande R, Butrico L, Rossi A, Settimio UF, Caroleo B, Amato B, Gallelli L, De Franciscis S. 2015. Chronic wound infections: The role of Pseudomonas aeruginosa and Staphylococcus aureus. Expert Rev Anti Infect Ther 13:605–613.

13. Moran GJ, Krishnadasan A, Gorwitz RJ, Fosheim GE, McDougal LK, Carey RB, Talan DA. 2006. Methicillin-Resistant S. aureus Infections among Patients in the Emergency Department. N Engl J Med 355:666–674.

14. Thurlow LR, Stephens AC, Hurley KE, Richardson AR. 2020. Lack of nutritional immunity in diabetic skin infections promotes Staphylococcus aureus virulence.

15. Jacquet R, LaBauve AE, Akoolo L, Patel S, Alqarzaee AA, Fok Lung TW, Poorey K, Stinear TP, Thomas VC, Meagher RJ, Parker D. 2019. Dual gene expression analysis identifies factors associated with Staphylococcus aureus virulence in diabetic mice. Infect Immun 87:1–18.

16. Gjødsbøl K, Christensen JJ, Karlsmark T, Jørgensen B, Klein BM, Krogfelt KA. 2006. Multiple bacterial species reside in chronic wounds□: a longitudinal study 3.

17. Trøstrup H, Lerche CJ, Christophersen LJ, Thomsen K, Jensen PØ, Hougen HP, Høiby N, Moser C. 2017. Chronic Pseudomonas aeruginosa biofilm infection impairs murine S100A8/A9 and neutrophil effector cytokines-implications for delayed wound closure? Pathog Dis 75:1–39.

18. Maeda H, Akaike T, Sakata Y, Maruo K. 1993. Role of Bradykinin in Microbial Infection: Enhancement of Septicemia by Microbial Proteases and Kinin, p. 159–165. *In* Proteases, Protease Inhibitors and Protease-Derived Peptides. Birkhäuser Basel, Basel.

19. Hidekatsu Yanai. 2012. Group B streptococcus infection and diabetes: A review. J Microbiol Antimicrob 4:1–5.

20. Schwartz B, Schuchat A, Oxtoby MJ, Cochi SL, Hightower A, Broome C V. 1991. Invasive Group B Streptococcal Disease in Adults: A Population-Based Study in Metropolitan Atlanta. JAMA J Am Med Assoc 266:1112–1114.

21. Regan JA, Klebanoff MA, Nugent RP. 1991. The epidemiology of group B streptococcal colonization in pregnancy. Vaginal Infections and Prematurity Study Group. Obstet Gynecol.

22. Wilkinson HW. 1978. Group b streptococcal infection in humans. Annu Rev Microbiol 41–57.

23. Gaschignard J, Levy C, Romain O, Cohen R, Bingen E, Aujard Y, Boileau P. 2011. Neonatal Bacterial Meningitis. Pediatr Infect Dis J 30:212–217.

24. Skoff TH, Farley MM, Petit S, Craig AS, Schaffner W, Gershman K, Harrison LH, Lynfield R, Mohle-boetani J, Zansky S, Albanese BA, Stefonek K, Zell ER, Jackson D, Thompson T, Schrag SJ. 2009. Increasing Burden of Invasive Group B Streptococcal Disease in Nonpregnant Adults , 1990 – 2007 30333:85–92.

25. Rosa-Fraile M, Dramsi S, Spellerberg B. 2014. Group B streptococcal haemolysin and pigment, a tale of twins. FEMS Microbiol Rev 38:932–946.

26. Buscetta M, Firon A, Pietrocola G, Biondo C, Mancuso G, Midiri A, Romeo L, Galbo R, Venza M, Venza I, Kaminski PA, Gominet M, Teti G, Speziale P, Trieu-Cuot P, Beninati C. 2016. PbsP, a cell wall-anchored protein that binds plasminogen to promote hematogenous dissemination of group B Streptococcus. Mol Microbiol 101:27–41.

27. Patras KA, Derieux J, Al-Bassam MM, Adiletta N, Vrbanac A, Lapek JD, Zengler K, Gonzalez DJ, Nizet V. 2018. Group B Streptococcus Biofilm Regulatory Protein A Contributes to Bacterial Physiology and Innate Immune Resistance. J Infect Dis 218:1641–1652.

28. Armistead B, Oler E, Waldorf KA, Rajagopal L, Disease I. 2019. The double life of Group B Streptococcus: Asymptomatic colonizer and potent pathogen. J Mol Biol 431:2914–2931.

29. Deng L, Spencer BL, Holmes JA, Mu R, Rego S, Weston TA, Hu Y, Sanches GF, Yoon S, Park N, Nagao PE, Jenkinson HF, Thornton JA, Seo KS, Nobbs AH, Doran KS. 2019. The group B streptococcal surface antigen I/II protein, BspC, interacts with host vimentin to promote adherence to brain endothelium and inflammation during the pathogenesis of meningitis. PLoS Pathog 15:1–30.

30. Edmond KM, Kortsalioudaki C, Scott S, Schrag SJ, Zaidi AKM, Cousens S, Heath PT. Group B streptococcal disease in infants aged younger than 3 months□: systematic review and meta-analysis. Lancet 379:547–556.

31. Beier D, Gross R. 2006. Regulation of bacterial virulence by two-component systems. Curr Opin Microbiol 9:143–152.

32. Jiang S, Cieslewicz MJ, Kasper DL, Wessels MR. 2005. Regulation of Virulence by a

Two-Component System in Group B Streptococcus † 187:1105–1113.

33. Faralla C, Metruccio MM, De Chiara M, Mu R, Patras KA, Muzzi A, Grandi G, Margarit I, Doran KS, Janulczyk R. 2014. Analysis of two-component systems in group B streptococcus shows that RgfAC and the novel FspSR modulate virulence and bacterial fitness. MBio 5:1–12.

34. Lamy M, Zouine M, Fert J, Vergassola M, Couve E, Pellegrini E, Glaser P, Kunst F, Msadek T, Trieu-cuot P, Poyart C. 2004. CovS / CovR of group B streptococcus□: a two-component global regulatory system involved in virulence 54:1250–1268.

35. Patras KA, Wang NY, Fletcher EM, Cavaco CK, Jimenez A, Garg M, Fierer J, Sheen TR, Rajagopal L, Doran KS. 2013. Group B Streptococcus CovR regulation modulates host immune signalling pathways to promote vaginal colonization. Cell Microbiol 15:1154–1167.

36. Lembo A, Gurney MA, Burnside K, Banerjee A, De M, Reyes L, Connelly JE, Lin W, Jewell KA, Vo A, Renken CW, Doran KS, Rajagopal L. 2010. Regulation of CovR expression in Group B streptococcus impacts blood-brain barrier penetration. Mol Microbiol 77:431–443.

37. Mandel MA, Mahmoud AA. 1978. Impairment of cell-mediated immunity in mutation diabetic mice (db/db). J Immunol 120:1375–1377.

38. P. HK, M. DM, L. CD. 1966. Diabetes, a New Mutation in the Mouse. Science (80-) 153:1127–1128.

39. Edwards JM, Watson N, Focht C, Wynn C, Todd CA, Walter EB, Phillips Heine R,

Swamy GK. 2019. Group B Streptococcus (GBS) Colonization and Disease among Pregnant Women: A Historical Cohort Study. Infect Dis Obstet Gynecol 2019.

40. Poyart C, Tazi A, Réglier-Poupet H, Billoët A, Tavares N, Raymond J, Trieu-Cuot P. 2007. Multiplex PCR assay for rapid and accurate capsular typing of group B streptococci. J Clin Microbiol 45:1985–1988.

41. Deng L, Schilcher K, Burcham LR, Kwiecinski JM, Johnson PM, Head SR. 2019. Identification of Key Determinants of Staphylococcus aureus Vaginal Colonization 1–19.

42. Rahn S, Zimmermann V, Viol F, Knaack H, Stemmer K, Peters L, Lenk L, Ungefroren H, Saur D, Schäfer H, Helm O, Sebens S. 2018. Diabetes as risk factor for pancreatic cancer: Hyperglycemia promotes epithelial-mesenchymal-transition and stem cell properties in pancreatic ductal epithelial cells. Cancer Lett 415:129–150.

43. Lombardi A, Tsomos E, Hammerstad SS, Tomer Y. 2018. Interferon alpha: The key trigger of type 1 diabetes. J Autoimmun 94:7–15.

44. Fabregat A, Sidiropoulos K, Viteri G, Forner O, Marin-Garcia P, Arnau V, D'Eustachio P, Stein L, Hermjakob H. 2017. Reactome pathway analysis: A high-performance in-memory approach. BMC Bioinformatics 18:1–9.

45. Jiang SM, Ishmael N, Hotopp JD, Puliti M, Tissi L, Kumar N, Cieslewicz MJ, Tettelin H, Wessels MR. 2008. Variation in the group B Streptococcus CsrRS regulon and effects on pathogenicity. J Bacteriol 190:1956–1965.

46. Mazzuoli MV, Daunesse M, Varet H, Rosinski-Chupin I, Legendre R, Sismeiro O, Gominet M, Kaminski PA, Glaser P, Chica C, Trieu-Cuot P, Firon A. 2021. The CovR

regulatory network drives the evolution of Group B Streptococcus virulence. PLoS Genet 17:1–27.

47. Rajagopal L. 2009. Understanding the regulation of Group B Streptococcal virulence factors. Future Microbiol 4:201–221.

48. Lupo A, Ruppen C, Hemphill A, Spellerberg B, Sendi P. 2014. Phenotypic and molecular characterization of hyperpigmented group B Streptococci. Int J Med Microbiol 304:717–724.

49. Whidbey C, Burnside K, Martinez RM, Gendrin C, Frando A, Harrell MI, Mcadams R. 2015. A Hyperhemolytic/Hyperpigmented Group B Streptococcus Strain with a CovR Mutation Isolated from an Adolescent Patient with Sore Throat. Clin Res Infect Dis 2:1–12.

50. Doran KS, Chang JCW, Benoit VM, Eckmann L, Nizet V. 2002. Group B streptococcal β-hemolysin/cytolysin promotes invasion of human lung epithelial cells and the release of interleukin-8. J Infect Dis 185:196–203.

51. Liu GY, Doran KS, Lawrence T, Turkson N, Puliti M, Tissi L, Nizet V. 2004. Sword and shield: Linked group B streptococcal β-hemolysin/cytolysin and carotenoid pigment function to subvert host phagocyte defense. Proc Natl Acad Sci U S A 101:14491–14496.

52. Armistead B, Herrero-Foncubierta P, Coleman M, Quach P, Whidbey C, Justicia J, Tapia R, Casares R, Millán A, Haidour A, Granger JR, Vornhagen J, Santana-Ufret V, Merillat S, Adams Waldorf K, Cuerva JM, Rajagopal L. 2020. Lipid analogs reveal features critical for hemolysis and diminish granadaene mediated Group B Streptococcus infection. Nat Commun 11:1502.

53. Papasergi S, Galbo R, Lanza-Cariccio V, Domina M, Signorino G, Biondo C, Pernice I, Poyart C, Trieu-Cuot P, Teti G, Beninati C. 2013. Analysis of the Streptococcus agalactiae exoproteome. J Proteomics 89:154–164.

54. Lentini G, Midiri A, Firon A, Galbo R, Mancuso G, Biondo C, Mazzon E, Passantino A, Romeo L, Trieu-Cuot P, Teti G, Beninati C. 2018. The plasminogen binding protein PbsP is required for brain invasion by hypervirulent CC17 Group B streptococci. Sci Rep 8:1–11.

55. De Gaetano GV, Pietrocola G, Romeo L, Galbo R, Lentini G, Giardina M, Biondo C, Midiri A, Mancuso G, Venza M, Venza I, Firon A, Trieu-Cuot P, Teti G, Speziale P, Beninati C. 2018. The Streptococcus agalactiae cell wall-anchored protein PbsP mediates adhesion to and invasion of epithelial cells by exploiting the host vitronectin/αvintegrin axis. Mol Microbiol 110:82–94.

56. Dickson MA, Hahn WC, Ino Y, Ronfard V, Wu JYd, Weinberg R a, Louis DN, Li FP, Rheinwald JG. 2000. Human Keratinocytes That Express hTERT and Also Bypass a p16 INK4a -Enforced Mechanism That Limits Life Span Become Immortal yet Retain Normal Growth and Differentiation Characteristics. Mol Cell Biol 20:1436–1447.

57. Wong SL, Demers M, Martinod K, Gallant M, Wang Y, Goldfine AB, Kahn CR, Wagner DD. 2015. Diabetes primes neutrophils to undergo NETosis, which impairs wound healing. Nat Med 21:815–819.

58. Hanses F, Park S, Rich J, Lee JC. 2011. Reduced neutrophil apoptosis in diabetic mice during staphylococcal infection leads to prolonged Tnfα production and reduced neutrophil clearance. PLoS One 6.

59. Jones SG, Edwards R, Thomas DW. 2004. Inflammation and Wound Healing: The Role of Bacteria in the Immuno-Regulation of Wound Healing. Int J Low Extrem Wounds 3:201–208.

60. Wennekamp J, Henneke P. 2008. Induction and termination of inflammatory signaling in group B streptococcal sepsis. Immunol Rev 225:114–127.

61. Sumitomo T, Nakata M, Higashino M, Yamaguchi M, Kawabata S. 2016. Group A Streptococcus exploits human plasminogen for bacterial translocation across epithelial barrier via tricellular tight junctions. Sci Rep 7:1–8.

62. Guo Y, Li J, Hagström E, Ny T. 2011. Beneficial and detrimental effects of plasmin(Ogen) during infection and sepsis in mice. PLoS One 6.

63. Shen Y, Guo Y, Mikus P, Sulniute R, Wilczynska M, Ny T, Li J. 2012. Plasminogen is a key proinflammatory regulator that accelerates the healing of acute and diabetic wounds. Blood 119:5879–5887.

64. Cook LCC, Hu H, Maienschein-cline M, Federle J. 2018. A Vaginal Tract Signal Detected by the Group B Streptococcus SaeRS System Elicits Transcriptomic Changes and Enhances. Infect Immun 1–17.

65. Kroeze K, Gibbs S. 2012. Comparison of cytokine , chemokine and growth factor profiles in burn wounds , chronic wounds and surgical excision wounds.

66. Derré-Bobillot A, Cortes-Perez NG, Yamamoto Y, Kharrat P, Couvé E, Da Cunha V, Decker P, Boissier MC, Escartin F, Cesselin B, Langella P, Bermúdez-Humarán LG, Gaudu P. 2013. Nuclease A (Gbs0661), an extracellular nuclease of Streptococcus

agalactiae, attacks the neutrophil extracellular traps and is needed for full virulence. Mol Microbiol 89:518–531.

67. Trends C, Directions F. 2021. Wound Healing ResearchWound Healing Research.

68. Hotterbeekx A, Kumar-Singh S, Goossens H, Malhotra-Kumar S. 2017. In vivo and In vitro interactions between Pseudomonas aeruginosa and Staphylococcus spp. Front Cell Infect Microbiol 7:1–13.

69. Pérez-Pascual D, Gaudu P, Fleuchot B, Besset C, Rosinski-Chupin I, Guillot A, Monnet V, Gardan R. 2015. RovS and its associated signaling peptide form a cell-to-cell communication system required for Streptococcus agalactiae pathogenesis. MBio 6.

70. Cook LC, LaSarre B, Federle MJ. 2013. Interspecies communication among commensal and pathogenic streptococci. MBio 4.

71. Sendi P, Johansson L, Dahesh S, Van Sorge NM, Darenberg J, Norgren M, Sjölin J, Nizet V, Norrby-Teglund A. 2009. Bacterial phenotype variants in group B streptococcal toxic shock syndrome. Emerg Infect Dis 15:223–232.

72. Walker MJ, Hollands A, Sanderson-Smith ML, Cole JN, Kirk JK, Henningham A, McArthur JD, Dinkla K, Aziz RK, Kansal RG, Simpson AJ, Buchanan JT, Chhatwal GS, Kotb M, Nizet V. 2007. DNase Sda1 provides selection pressure for a switch to invasive group A streptococcal infection. Nat Med 13:981–985.

73. Sumby P, Whitney AR, Graviss EA, DeLeo FR, Musser JM. 2006. Genome-wide analysis of group A streptococci reveals a mutation that modulates global phenotype and disease specificity. PLoS Pathog 2:0041–0049.

74. Love MI, Huber W, Anders S. 2014. Moderated estimation of fold change and dispersion for RNA-seq data with DESeq2. Genome Biol 15:1–21.

75. Liberzon A, Subramanian A, Pinchback R, Thorvaldsdóttir H, Tamayo P, Mesirov JP. 2011. Molecular signatures database (MSigDB) 3.0. Bioinformatics 27:1739–1740.

76. Spencer BL, Deng L, Patras KA, Burcham ZM, Sanches GF, Nagao PE, Doran KS. 2019. Cas9 contributes to group b streptococcal colonization and disease. Front Microbiol 10:1–15.

77. Flores AR, Galloway-Peña J, Sahasrabhojane P, Saldaña M, Yao H, Su X, Ajami NJ, Holder ME, Petrosino JF, Thompson E, Ros IMY, Rosini R, Grandi G, Horstmann N, Teatero S, McGeer A, Fittipaldi N, Rappuoli R, Baker CJ, Shelburne SA. 2015. Sequence type 1 group B Streptococcus, an emerging cause of invasive disease in adults, evolves by small genetic changes. Proc Natl Acad Sci U S A 112:6431–6436.

78. Madoff LC, Michel JL, Kasper DL. 1991. A monoclonal antibody identifies a protective C-protein alpha-antigen epitope in Group B streptococci. Infect Immun 59:204–210.

79. Wilson CB, Weaver WM. 1985. Comparative Susceptibility of Group B Streptococci and Staphylococcus aureus to Killing by Oxygen Metabolites. J Infect Dis 152:323–329.